CTU Journal of Innovation and Sustainable Development
ISSN 2615-9422 | e-ISSN 2815-5602

DOI:10.22144/ctujoisd.2024.265

Outage probability of cognitive radio-NOMA assisted unmanned aerial vehicles network

Dan Le Quoc, Nhat Tien Nguyen*, and Nguyen Thi Thu Hang

Faculty of Electronics and Telecommunications, Saigon University, Viet Nam

**Corresponding author (tien.nn@sgu.edu.vn)*

Article info.

Received 10 Sep 2023
Revised 18 Oct 2023
Accepted 30 Oct 2023

Keywords

Non-orthogonal multiple access, outage performance, unmanned aerial vehicle

ABSTRACT

Unmanned aerial vehicles have been applied and play a critical role in radio surveillance because of their flexibility, mobility, and likely line-of-sight to ground destinations. Here, UAVs provide LoS links to users in the communication shadow of obstructive buildings. This paper investigates a cognitive radio network system model between unmanned aerial vehicles to transfer information from a licensed primary device to unlicensed users in a secondary network. In which PN users rely on non-orthogonal multiple access to prevent interference with each other. The primary objective of this study is to examine the outage probability of the secondary users with perfect and imperfect successive interference cancellation applications. Finally, we derive the users' exact closed-form expressions and use Monte Carlo simulations to validate the analytical results.

1. INTRODUCTION

Unmanned aerial vehicles (UAVs) have acquired enormous popularity in numerous areas of society ranging from food delivery to wireless communication (Hayat et al., 2016). In wireless communication, they find UAVs the best use as aerial base stations to provide short-range line-of-sight (LoS) linkage between base stations and obstructed ground users. UAVs present a potential opportunity to implement flying base stations (BSs) mounted on UAVs that have the ability to autonomously adjust their positions to enhance coverage, spectral efficiency, and user quality of experience (Fotouhi et al., 2019). Ways in which drones can enhance the operation of the wireless network include enhancing capacity as needed, extending coverage range, and enhancing reliability and agility as an aerial node. In (Bor-Yaliniz et al., 2019), the authors investigated two cases of mobile-enabled drones (MEDs) and wireless infrastructure drones (WIDs). There have been many good survey papers and tutorials written on the subject of UAV cellular communications such as Zhang et al. (2019), Shi et al. (2018), Mozaffari et al. (2019), and Zeng et al. (2016).

The UAVs operate as an aerial base station, connecting two ground users in a secondary network (SN). This SN network is part of a cooperative cognitive radio network (CRN). The CRN aims to provide spectrum access to as various users as possible, regardless of whether they are licensed or unlicensed. According to Letaief et al. (2009), Yucek et al. (2009), and Liang et al. (2011), cognitive radio (CR) is seen as a promising solution to tackle the issue of limited spectrum in upcoming wireless networks. Standardization organizations have made considerable efforts to achieve CR technology (Liang et al., 2011); Sharma et al., 2015, part I and II, pp. 3388–3391). Moreover, the CRN needs to guarantee that interference levels are kept below a specific threshold to prevent any disruption to either the primary network (PN) or the cognitive radio network itself (Do et al., 2020). We further integrate the CRN with non-orthogonal multiple access (NOMA).

NOMA technology is a promising option for improving spectral efficiency (SE) as it can cater to multiple wireless users at the same time by combining them in either power or code domains (Arzykulov et al., 2021). Integrating NOMA with CRs shows great promise for UAV cellular networks. In collaborative CR-supported NOMA, a UAV relay station that has a clear LoS capability decodes and relays messages meant for users with weaker signals affected by shadowing in order to maintain the quality-of-service (QoS) standards of the network (Nguyen et al., 2022). Therefore, the combination of CR-NOMA and UAV promises to provide greater service coverage compared to traditional fixed relays.

To satisfy the capacity of UAV-assisted wireless networks and the demands of the highest data rate, the downlink and uplink of the cooperative CR-NOMA assisted by UAVs must be carefully designed. In the development of cooperative CR-NOMA solutions, it is essential to consider power allocation, hardware capabilities for successive interference cancellation (SIC), user clustering/pairing, and primary network interference (Do et al., 2022). In Tang et al. (2020), Arzykulov et al. (2021), and Zhang et al. (2021), the authors explore aspects related to clustering, primary network interference, and resource allocation. Moreover, the researchers develop an equitable optimization framework for power control and phase-time allocation in cooperative CR-NOMA with the assistance of UAVs. However, in the studies of Arzykulov et al. (2018), Tang et al. (2020), and Luo et al. (2020), the outage performances of the system are not considered. Inspired by the need for optimal research with the system model, our primary contributions are the following:

– First, the precise expressions for the outage probability (OP) of the secondary network users are obtained.

– Second, we examine the impact of SIC and the altitude of the UAV on the OP from these expressions.

All statements are confirmed through Monte Carlo simulations.

The structure of the paper is as follows. Section 2 presents the system parameters. Following that, Section 3 provides closed-form expressions for OP. Section 4 discusses the results and includes a summary in Section 5.

2. COOPERATIVE CR-NOMA ASSISTED UAV WIRELESS NETWORK MODEL

We consider a UAV cooperative NOMA-CR network which comprises a secondary network (SN) and a primary network (PN). We assume a UAV (U), two secondary devices D_1, D_2, and a primary device (PD) as in Figure 1. Moreover, g_1, g_2 and g_{UP} define the Nakagami-m channel fading between U and D_1, U and D_2 and U and PD, respectively.

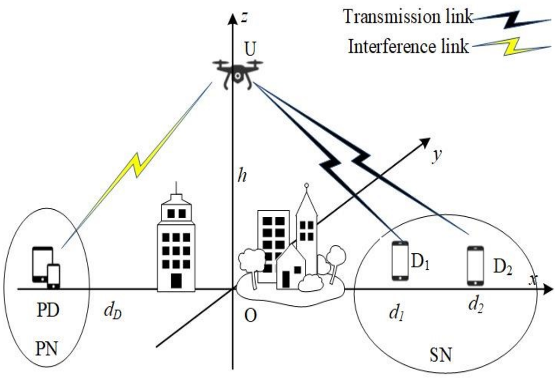

Figure 1. UAV-aided NOMA network system model

In Figure 1, we consider three-dimensional cartesian coordinates (x, y, z). First, we present the location of the UAV (U) at $U(0,0,h)$. Then, we present the ground users D_1 and D_2 which are at $D_1(d_1,0,0)$ and $D_2(d_2,0,0)$. Further, we assume the location of the primary destination at $PD(-d_D,0,0)$.

$$d_{UD_i} = \sqrt{d_i^2 + h^2} \tag{1}$$

Moreover, the distance between U and PD is given as

$$d_{UP} = \sqrt{d_D^2 + h^2} \tag{2}$$

The power at U is limited as [21]

$$P_U = \min\left(\frac{P_p d_{UP}^m}{|g_{UP}|^2}, P_U^{\max}\right) \tag{3}$$

where P_p is the interference constraint, m is the path-loss exponent and $P_U^{\max}$ is the maximum transmit power at U. Moreover, U transmit the message $s_U = \alpha_1 s_1 + \alpha_2 s_2$ to D_i with $i \in \{1,2\}$, where s_i is the message of D_i, α_i is the power allocation coefficient and $\alpha_1 < \alpha_2$. The received signal at D_i is given by

$$s_{D_i} = \sqrt{\frac{P_U}{d_{UD_i}^m}} g_i(\alpha_1 s_1 + \alpha_2 s_2) + n_i \tag{4}$$

where $n_i \sim (0, \sigma_i^2)$ denotes the AWGN with zero mean and variance σ_i^2. The signal-to-interference-plus-noise ratio (SINR) to enable D_2 to detect s_2 and reject s_1 as interference is given by

$$SINR_{D_2 \to s_2} = \frac{P_U |g_2|^2 \alpha_2^2}{P_U |g_2|^2 \alpha_1^2 + d_{UD_2}^m \alpha_2^2} = \frac{\mu_U |g_2|^2 \alpha_2^2}{\mu_U |g_2|^2 \alpha_1^2 + d_{UD_2}^m} \tag{5}$$

where $\mu_U = \frac{P_U}{\sigma_i^2}$. First, D_1 detects the signal s_2 and the SINR is given by

$$SINR_{D_1 \to s_2} = \frac{\mu_U |g_1|^2 \alpha_2^2}{\mu_U |g_1|^2 \alpha_1^2 + d_{UD_1}^m} \tag{6}$$

Next, successive interference cancellation (SIC) is implemented (Do et al., 2019) to detect the signal s_1 of D_1 and the SINR is given by

$$SINR_{D_1 \to s_1}^{ipSIC} = \frac{\mu_U |g_1|^2 \alpha_1^2}{\mu_U \varpi |g_I|^2 + d_{UD_1}^m} \tag{7}$$

where $\varpi = 0$ denotes the pSIC and $\varpi = 1$ denotes the ipSIC. Moreover, g_I^2 is the rayleigh fading channel with $CN(0, \lambda_I)$ (Kader et al., 2017).

Here, the channel g_p where $p \in \{1,2,UP\}$ can be modeled by (Ji et al., 2019)

$$f_{|g_p|^2}(x) = \frac{x^{m_p - 1} \beta_p^{m_p}}{\Gamma(m_p)} e^{-\beta_p x} \tag{8}$$

where $\beta_p = \frac{m_p}{\lambda_p}$, λ_p is the average power, m_p is the fading severity and $\Gamma(.)$ is the gamma function.

3. OUTAGE PERFORMANCE

3.1. Outage probability of D_2

The outage events of D_2 occur when D_2 cannot successfully detect the signal x_2. Therefore, the OP of D_2 is expressed as.

$$P_{D_2} = 1 - \Pr(SINR_{D_2 \to s_2} > \vartheta_2) \tag{9}$$

Where are the threshold and ϑ_2 the target rate of D_i .

Proposition 1: The closed-form OP of D_2 is given by

$$\begin{aligned} P_{D_2} = 1 &- \frac{\Gamma\left(m_2, \frac{\beta_2\theta_2}{\tilde{\mu}_U} \gamma\left(m_{UP}, \frac{\beta_{UP}\mu_I d_{UP}^m}{\tilde{\mu}_U}\right)\right)}{\Gamma(m_2)\Gamma(m_{UP})} \\ &- \sum_{a=0}^{m_2-1} \frac{\left(\beta_{UP}\mu_I d_{UP}^m\right)^{m_{UP}} \left(\beta_2\theta_2\right)^a}{a!\Gamma(m_{UP})(\beta_{UP}\mu_I d_{UP}^m + \beta_2\theta_2)^{m_{UP}+a}} \\ &\times \Gamma\left(m_{UP} + a, \frac{\beta_{UP}\mu_I d_{UP}^m + \beta_2\theta_2}{\tilde{\mu}_U}\right). \end{aligned} \tag{10}$$

Proof:

With help (3) and (5), $P_{D_2}^{OP}$ can be rewrite as follow

$$\begin{aligned} P_{D_2} = 1 &- \underbrace{\Pr\left(\frac{\tilde{\mu}_U |g_2|^2 \alpha_2^2}{\tilde{\mu}_U |g_2|^2 \alpha_1^2 + d_{UD_2}^m} > \vartheta_2, |g_{UP}|^2 < \frac{\mu_1 d_{UP}^m}{\tilde{\mu}_U}\right)}_{A_1} \\ &+ \underbrace{\Pr\left(\frac{\frac{\mu_I d_{UP}^m}{|g_{UP}|^2} |g_2|^2 \alpha_2^2}{\frac{\mu_I d_{UP}^m}{|g_{UP}|^2} |g_2|^2 \alpha_1^2 + d_{UD_2}^m} > \vartheta_2, |g_{UP}|^2 > \frac{\mu_1 d_{UP}^m}{\tilde{\mu}_U}\right)}_{A_2} \end{aligned} \tag{11}$$

where $\mu_I = \frac{P_p}{\sigma^2}$ and $\tilde{\mu}_U = \frac{P_U^{max}}{\sigma^2}$. Then, the term A_1 of (11) is calculated as

$$A_1 = \Pr\left(| g_2 |^2 > \frac{\theta_2}{\tilde{\mu}_U}, | g_{UP} |^2 < \frac{\mu_I d_{UP}^m}{\tilde{\mu}_U} \right) = \int_{\frac{\theta_2}{\tilde{\mu}_U}}^{\infty} f_{|g_2|^2}(x) \int_0^{\frac{\mu_I d_{UP}^m}{\tilde{\mu}_U}} f_{|g_{UP}|^2}(y) dx dy \tag{12}$$

where $\theta_2 = \frac{\vartheta_2 d_{UD_2}^m}{\alpha_2^2 - \vartheta_S \alpha_1^2}$. Base on (8) and [Gradshteyn et al., 2014, 3.351] A_1 can be obtained by

$$A_1 = \frac{\beta_2^{m_2} \beta_{UP}^{m_{UP}}}{\Gamma(m_2)\Gamma(m_{UP})} \int_{\frac{\theta_2}{\tilde{\mu}_U}}^{\infty} x^{m_2-1} e^{-\beta_2 x} \int_0^{\frac{\mu_I d_{UP}^m}{\tilde{\mu}_U}} y^{m_{UP}-1} e^{-\beta_{UP} y} dx dy = \frac{1}{\Gamma(m_2)\Gamma(m_{UP})} \Gamma\left(m_2, \frac{\beta_2 \theta_2}{\tilde{\mu}_U} \right) \gamma\left(m_{UP}, \frac{\beta_{UP} \mu_I d_{UP}^m}{\tilde{\mu}_U} \right). \tag{13}$$

where $\Gamma(.,.)$ and $\gamma(.,.)$ are the incomplete gamma function (Gradshteyn et al., 2014)[25] A_2 of (11) is rewritten as.

$$A_2 = \Pr\left(|g_2|^2 > \frac{\theta_2 |g_{UP}|^2}{\mu_I d_{UP}^m}, |g_{UP}|^2 > \frac{\mu_I d_{UP}^m}{\tilde{\mu}_U} \right) = \int_{\frac{\mu_I d_{UP}^m}{\tilde{\mu}_U}}^{\infty} f_{|g_{UP}|^2}(x) \int_{\frac{\theta_2 x}{\mu_I d_{UP}^m}}^{\infty} f_{|g_2|^2}(y) dy dx \tag{14}$$

Putting (8) into (14) and using [Gradshteyn et al., 2014, 3.351.2], we have

$$A_2 = \frac{\beta_2^{m_2} \beta_{UP}^{m_{UP}}}{\Gamma(m_2)\Gamma(m_{UP})} \int_{\frac{\mu_I d_{UP}^m}{\tilde{\mu}_U}}^{\infty} x^{m_{UP}-1} e^{-\beta_{UP} x} \int_{\frac{\theta_2 x}{\mu_I d_{UP}^m}}^{\infty} y^{m_2-1} e^{-\beta_2 y} dy dx = \sum_{a=0}^{m_2-1} \frac{\beta_{UP}^{m_{UP}}}{a!\Gamma(m_{UP})} \left(\frac{\beta_2 \theta_2}{\mu_I d_{UP}^m} \right)^a \int_{\frac{\mu_I d_{UP}^m}{\tilde{\mu}_U}}^{\infty} x^{m_{UP}+a-1} e^{-\beta_{UP} x - \frac{\beta_2 \theta_2}{\mu_I d_{UP}^m} x} dx \tag{15}$$

Moreover, A_2 can be obtained by

$$A_2 = \sum_{a=0}^{m_2-1} \frac{\left(\beta_{UP} \mu_I d_{UP}^m \right)^{m_{UP}} \left(\beta_2 \theta_2 \right)^a}{a!\Gamma(m_{UP}) \left(\beta_{UP} \mu_I d_{UP}^m + \beta_2 \theta_2 \right)^{m_{UP}+a}} \times \Gamma\left(m_{UP} + a, \frac{\beta_{UP} \mu_I d_{UP}^m + \beta_2 \theta_2}{\tilde{\mu}_U} \right) \tag{16}$$

Substituting (13) and (16) into (11), (10) is obtain and the proof is complete.

3.2. Outage probability D_1

The outage events of D_1 occur when the signal x_2 cannot be detected by and cannot detect x_1. So, the outage probability of D_1 is given by.

$$P_{D_1}^{ipSIC} = 1 - \Pr(SINR_{D_1 \to s_2} > \vartheta_2, SINR_{D_1 \to s_2} > \vartheta_1) \tag{17}$$

Proposition 2: The closed-form outage probability of D_1 is given by

$$\begin{aligned} P_{D_1}^{ipSIC} = 1 - & \frac{\gamma\left(m_{UP}, \frac{\beta_{UP} \mu_I d_{UP}^m}{\tilde{\mu}_U} \right)}{\Gamma(m_{UP})\Gamma(m_1)} \left(\Gamma\left(m_1, \frac{\beta_1 \theta_{\max}}{\tilde{\mu}_U} \right) - \frac{e^{\frac{d_{UD_1}^m}{\lambda_I \tilde{\mu}_U \varpi}} \Gamma\left(m_1, \frac{\psi \beta_1 \theta_{\max}}{\tilde{\mu}_U} \right)}{\psi^{m_1}} \right) \\ & - \sum_{n=0}^{m_1-1} \frac{\left(\frac{\beta_1 \theta_{\max}}{\beta_{UP} \mu_I d_{UP}^m} \right)^n}{n!\Gamma(m_{UP})} \left(1 + \frac{\beta_1 \theta_{\max}}{\beta_{UP} \mu_I d_{UP}^m} \right)^{-m_{UP}-n} \Gamma\left(m_{UP} + n, \frac{\beta_{UP} \mu_I d_{UP}^m + \beta_1 \theta_{\max}}{\tilde{\mu}_U} \right) \\ & + \sum_{n=0}^{m_1-1} \frac{\psi^{-m_1-m_{UP}}}{n!\Gamma(m_{UP})} \left(\frac{\beta_1 \theta_{\max}}{\beta_{UP} \mu_I d_{UP}^m} \right)^{m_{UP}} \left(1 + \frac{\beta_{UP} \mu_I d_{UP}^m}{\psi \beta_1 \theta_{\max}} - \frac{d_{UD_1}^m}{\lambda_I \varpi \psi \beta_1 \theta_{\max}} \right)^{-m_{UP}-n} \\ & \times \Gamma\left(m_{UP} + n, \left(\frac{\beta_{UP} \mu_I d_{UP}^m}{\tilde{\mu}_U} - \frac{d_{UD_1}^m}{\lambda_I \varpi \tilde{\mu}_U} + \frac{\psi \beta_1 \theta_{\max}}{\tilde{\mu}_U} \right) \right). \end{aligned} \tag{18}$$

Proof:

Putting (6) and (7) into (17), $P_{D_1}^{OP}$ is rewrite by

$$P_{D_1}^{ipSIC} = 1 - \underbrace{\Pr\left(|g_{D_1}|^2 > \frac{\theta_{\max}}{\tilde{\mu}_U}, |g_I|^2 < \frac{|g_1|^2 \alpha_1^2 \tilde{\mu}_U - \vartheta_1 d_{UD_1}^m}{\vartheta_1 \varpi \tilde{\mu}_U}, |g_{UP}|^2 < \frac{\mu_I d_{UP}^m}{\tilde{\mu}_U} \right)}_{B_1} - \underbrace{\Pr\left(|g_1|^2 > \frac{\theta_{\max} |g_{UP}|^2}{\mu_I d_{UP}^m}, |g_I|^2 < \frac{|g_{D_1}|^2 \alpha_1^2 \tilde{\mu}_U - \vartheta_1 d_{UD_1}^m}{\vartheta_1 \varpi \tilde{\mu}_U}, |g_{UP}|^2 > \frac{\mu_I d_{UP}^m}{\tilde{\mu}_U} \right)}_{B_2} \tag{19}$$

where $\theta_1 = \frac{\vartheta_2 d_{UD_1}^m}{\alpha_2^2 - \vartheta_2 \alpha_1^2}$, $\theta_3 = \frac{\vartheta_1 d_{UD_1}^m}{\alpha_1^2}$ and $\theta_{\max} = \max\left(\theta_1, \theta_3\right)$. Then, we can calculate B_1 as

$$B_1 = \int_{\frac{\theta_{\max}}{\tilde{\mu}_U}}^{\infty} f_{|g_1|^2}(x) \int_0^{\frac{x\alpha_1^2}{\vartheta_1\varpi} - \frac{d_{UD_1}^m}{\tilde{\mu}_U\varpi}} f_{|g_I|^2}(y) \int_0^{\frac{\mu_I d_{UP}^m}{\tilde{\mu}_U}} f_{|g_{UP}|^2}(z) dz dy dx$$
$$= \frac{\beta_1^{m_1}\gamma\left(m_{UP}, \frac{\beta_{UP}\mu_I d_{UP}^m}{\tilde{\mu}_U}\right)}{\Gamma(m_{UP})\Gamma(m_1)} \times \left(\int_{\frac{\theta_{\max}}{\tilde{\mu}_U}}^{\infty} x^{m_1-1} e^{-\beta_1 x} dx - e^{\frac{d_{UD_1}^m}{\lambda_I \tilde{\mu}_U \varpi}} \int_{\frac{\theta_{\max}}{\tilde{\mu}_U}}^{\infty} x^{m_1-1} e^{-\beta_1 x} e^{-\frac{x\alpha_1^2}{\lambda_I \vartheta_1 \varpi}} dx \right) \tag{20}$$

Similar in proposition 1, B_1 can be obtained by

$$B_1 = \frac{\gamma\left(m_{UP}, \frac{\beta_{UP}\mu_I d_{UP}^m}{\tilde{\mu}_U}\right)}{\Gamma(m_{UP})\Gamma(m_1)} \left(\Gamma\left(m_1, \frac{\beta_1\theta_{\max}}{\tilde{\mu}_U}\right) - \frac{e^{\frac{d_{UD_1}^m}{\lambda_I\tilde{\mu}_U\varpi}}}{\psi^{m_1}} \Gamma\left(m_1, \frac{\psi\beta_1\theta_{\max}}{\tilde{\mu}_U}\right) \right) \tag{21}$$

where $\psi = 1 + \frac{\alpha_1^2}{\beta_1\lambda_I\vartheta_1\varpi}$. Next, B_2 can be expressed as follows:

$$B_2 = \int_{\frac{\mu_I d_{UP}^m}{\tilde{\mu}_U}}^{\infty} f_{|g_{UP}|^2}(z) \int_{\frac{\theta_{\max} z}{\mu_I d_{UP}^m}}^{\infty} f_{|g_1|^2}(y) \int_0^{\frac{y\alpha_1^2}{\vartheta_1\varpi} - \frac{d_{UD_1}^m z}{\mu_I d_{UP}^m \varpi}} f_{|g_I|^2}(x) dx dy dz$$
$$= \underbrace{\int_{\frac{\mu_I d_{UP}^m}{\tilde{\mu}_U}}^{\infty} f_{|g_{UP}|^2}(z) \int_{\frac{\theta_{\max} z}{\mu_I d_{UP}^m}}^{\infty} f_{|g_1|^2}(y) dy dz}_{B_{2,1}}$$
$$\times \underbrace{\int_{\frac{\mu_I d_{UP}^m}{\tilde{\mu}_U}}^{\infty} f_{|g_{UP}|^2}(z) \int_{\frac{\theta_{\max} z}{\mu_I d_{UP}^m}}^{\infty} f_{|g_1|^2}(y) e^{-\left(\frac{y\alpha_1^2}{\lambda_I\vartheta_1\varpi} - \frac{d_{UD_1}^m z}{\lambda_I \mu_I d_{UP}^m \varpi}\right)} dy dz}_{B_{2,2}} \tag{22}$$

Putting (8) into (22), $B_{2,1}$ is given by

$$B_{2,1} = \frac{\beta_{UP}^{m_{UP}}\beta_1^{m_1}}{\Gamma(m_{UP})\Gamma(m_1)} \int_{\frac{\mu_I d_{UP}^m}{\tilde{\mu}_U}}^{\infty} z^{m_{UP}-1} e^{-\beta_{UP} z} \int_{\frac{\theta_{\max} z}{\mu_I d_{UP}^m}}^{\infty} y^{m_1-1} e^{-\beta_1 y} dy dz$$
$$= \sum_{n=0}^{m_1-1} \frac{1}{n!\Gamma(m_{UP})} \left(\frac{\beta_1\theta_{\max}}{\beta_{UP}\mu_I d_{UP}^m}\right)^n \left(1 + \frac{\beta_1\theta_{\max}}{\beta_{UP}\mu_I d_{UP}^m}\right)^{-m_{UP}-n} \times \Gamma\left(m_{UP}+n, \frac{\beta_{UP}\mu_I d_{UP}^m + \beta_1\theta_{\max}}{\tilde{\mu}_U}\right) \tag{23}$$

Similarly, the term $B_{2,2}$ can be expressed as follows

$$B_{2,2} = \frac{\beta_{UP}^{m_{UP}}\beta_1^{m_1}}{\Gamma(m_{UP})\Gamma(m_1)} \int_{\frac{\mu_I d_{UP}^m}{\tilde{\mu}_U}}^{\infty} z^{m_{UP}-1} e^{-\left(\beta_{UP} - \frac{d_{UD_1}^m}{\lambda_I\mu_I d_{UP}^m\varpi}\right)z} \int_{\frac{\theta_{\max} z}{\mu_I d_{UP}^m}}^{\infty} y^{m_1-1} e^{-\psi\beta_1 y} dy dz$$
$$= \sum_{n=0}^{m_1-1} \frac{\psi^{-m_1+n}\beta_{UP}^{m_{UP}}}{n!\Gamma(m_{UP})} \left(\frac{\beta_1\theta_{\max}}{\mu_I d_{UP}^m}\right)^n \int_{\frac{\mu_I d_{UP}^m}{\tilde{\mu}_U}}^{\infty} z^{m_{UP}+n-1} e^{-\left(\beta_{UP} - \frac{d_{UD_1}^m}{\lambda_I\mu_I d_{UP}^m\varpi}\right)z} e^{-\frac{\psi\beta_1\theta_{\max}}{\mu_I d_{UP}^m}z} dz$$
$$= \sum_{n=0}^{m_1-1} \frac{\left(\frac{\beta_1\theta_{\max}}{\beta_{UP}\mu_I d_{UP}^m}\right)^{m_{UP}}}{n!\Gamma(m_{UP})\psi^{m_1+m_{UP}}} \left(1 + \frac{\beta_{UP}\mu_I d_{UP}^m}{\psi\beta_1\theta_{\max}} - \frac{d_{UD_1}^m}{\lambda_I\varpi\psi\beta_1\theta_{\max}}\right)^{-m_{UP}-n} \times \Gamma\left(m_{UP}+n, \left(\frac{\beta_{UP}\mu_I d_{UP}^m}{\tilde{\mu}_U} - \frac{d_{UD_1}^m}{\lambda_I\varpi\tilde{\mu}_U} + \frac{\psi\beta_1\theta_{\max}}{\tilde{\mu}_U}\right)\right) \tag{24}$$

Finally, with help (21), (23) and (24). The closed-form outage probability of $P_{D_1}^{OP}$ is obtained.

The proof of proposition 2 is completed.

4. NUMERICAL RESULTS

4.1. Simulation main parameters

Here, we set the simulation main parameters as $\alpha_1^2 = 0.2$, $\alpha_2^2 = 0.8$, $m = 2$, $\lambda_1 = \lambda_2 = \lambda_{UP} = 1$, $m_1 = m_2 = m_{UP} = 2$, $\mu_I = 10[dB]$, $\lambda_I = 0.01$, $d_1 = d_D = 5m$, $d_1 = d_D = 5m$, $d_2 = h = 10m$ and $R_1 = R_2 = 0.5$ and $R_2 = 1$ bit per channel use.

4.2. Figures

Figure 2 illustrates the correlation between the OP and the UAV transmit SNR under various fading conditions $m_1 = m_2 = m_{UP}$. Eqs. (10) and (12) are utilized to create the analytical curves. By observing Figure 2, it is evident that the outage characteristics vary for secondary network users under different Nakagami-m fading scenarios. We also observe that at $\tilde{\mu}_U = 35dB$, OP of D_2 better than D_1. Moreover, the UAV transmit SNR stops impacting the OP. The analytical curves align closely with the Monte-Carlo simulations.

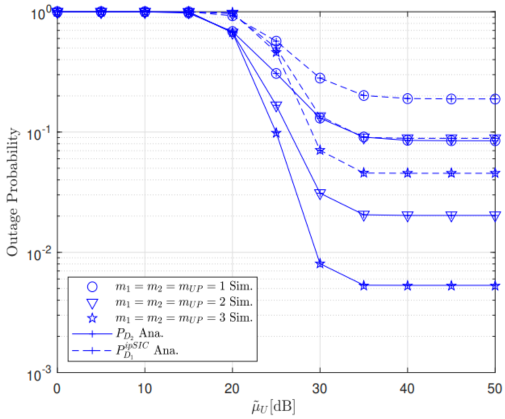

Figure 2. Outage probability versus $\tilde{\mu}_U[dB]$ varying m

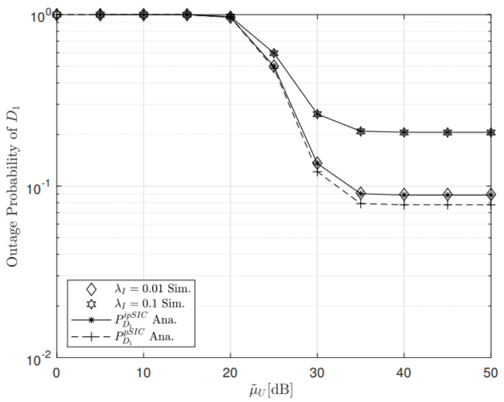

Figure 3. Outage probability of D_1 versus $\tilde{\mu}_U[dB]$ varying λ_I

Figure 3 illustrates the correlation between OP and UAV transmit SNR for various values. λ. From Figure 3, it is evident that the outage performance varies according to the value λ. We also observe a significant performance gap between pSIC and ipSIC, where the curve shows pSIC performing significantly better than ipSIC of D_1 at $\tilde{\mu}_U = 35dB$.

Finally, Figure 4 illustrates the correlation between OP and the altitude of the UAV, with different values of $\tilde{\mu}_U$. From Figure 4, it is evident that the height of the UAV has a notable impact on the OP. OP deteriorates as the UAV moves away from the users..

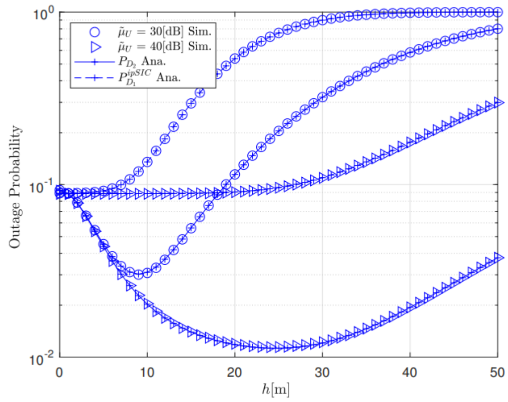

Figure 4. Outage probability versus $h[m]$ varying $\tilde{\mu}_U$

5. CONCLUSION

This article analyzed the outage probability in a UAV-assisted network employing NOMA protocol. We have obtained formulations for the outage probability for various users. Our focus lies on the performance of the distant user who requires the support of the UAV. The altitude and positioning of the UAV play a critical role in the outage performance of the distant user. The comparison is presented to highlight the contrast between the two users, which is determined by the power allocation factors they are assigned. In our future research, we will explore the system involving several UAVs.

ACKNOWLEDGMENT

The authors express their gratitude to the anonymous reviewers for their valuable comments and suggestions. This study is supported by Saigon University through the basic science research program CSB2023-08.

REFERENCES

Arzykulov, S., Tsiftsis, T. A., Nauryzbayev, G., & Abdallah, M. (2018). Outage performance of cooperative underlay CR-NOMA with imperfect CSI. *IEEE Communications Letters*, *23*(1), 176-179. https://doi.org/10.1109/LCOMM.2018.2878730

Arzykulov, S., Celik, A., Nauryzbayev, G., & Eltawil, A. M. (2021). UAV-assisted cooperative & cognitive NOMA: deployment, clustering, and resource allocation. *IEEE Transactions on Cognitive*

Communications and Networking, *8*(1), 263-281. https://doi.org/10.1109/TCCN.2021.3105133

Arzykulov, S., Celik, A., Nauryzbayev, G., & Eltawil, A. M. (2021). UAV-assisted cooperative & cognitive NOMA: deployment, clustering, and resource allocation. *IEEE Transactions on Cognitive Communications and Networking*, *8*(1), 263-281.

Bor-Yaliniz, I., Salem, M., Senerath, G., & Yanikomeroglu, H. (2019). Is 5G ready for drones: A look into contemporary and prospective wireless networks from a standardization perspective. *IEEE Wireless Communications*, *26*(1), 18-27. https://doi.org/10.1109/MWC.2018.1800229

Do, D. T., & Le, C. B. (2022). UAV-assisted underlay CR-NOMA network: performance analysis. Bulletin *of Electrical Engineering and Informatics*, *11*(4), 2079-2087. https://doi.org/10.1016/j.phycom.2020.101263

Do, D. T., Le, A. T., & Lee, B. M. (2020). NOMA in cooperative underlay cognitive radio networks under imperfect SIC. *IEEE Access*, *8*, 86180-86195. https://doi.org/10.1109/ACCESS.2020.2992660

Do, D. T., & Le, A. T. (2019). NOMA based cognitive relaying: Transceiver hardware impairments, relay selection policies and outage performance comparison. *Computer Communications*, *146*, 144-154.

Fotouhi, A., Qiang, H., Ding, M., Hassan, M., Giordano, L. G., Garcia-Rodriguez, A., & Yuan, J. (2019). Survey on UAV cellular communications: Practical aspects, standardization advancements, regulation, and security challenges. *IEEE Communications surveys & tutorials*, *21*(4), 3417-3442. https://doi.org/10.1109/COMST.2019.2906228

Gradshteyn, I. S., & Ryzhik, I. M. (2014). *Table of integrals, series, and products*. Academic press.

Hayat, S., Yanmaz, E., & Muzaffar, R. (2016). Survey on unmanned aerial vehicle networks for civil applications: A communications viewpoint. *IEEE Communications Surveys & Tutorials*, *18*(4), 2624-2661.

Ji, B., Li, Y., Zhou, B., Li, C., Song, K., & Wen, H. (2019). Performance analysis of UAV relay assisted IoT communication network enhanced with energy harvesting. *IEEE Access*, *7*, 38738-38747. https://doi.org/10.1109/ACCESS.2019.2906088

Kader, M. F., Shahab, M. B., & Shin, S. Y. (2017). Exploiting non-orthogonal multiple access in cooperative relay sharing. *IEEE Communications Letters*, *21*(5), 1159-1162. https://doi.org/10.1109/LCOMM.2017.2653777

Letaief, K. B., & Zhang, W. (2009). Cooperative communications for cognitive radio networks. *Proceedings of the IEEE*, *97*(5), 878-893. https://doi.org/10.1109/JPROC.2009.2015716

Liang, Y. C., Chen, K. C., Li, G. Y., & Mahonen, P. (2011). Cognitive radio networking and communications: An overview. *IEEE transactions on vehicular technology*, *60*(7), 3386-3407. https://doi.org/10.1109/TVT.2011.2158673

Luo, L., Li, Q., & Cheng, J. (2020). Performance analysis of overlay cognitive NOMA systems with imperfect successive interference cancellation. *IEEE Transactions on Communications*, *68*(8), 4709-4722. https://doi.org/10.1109/TCOMM.2020.2992471

Mozaffari, M., Saad, W., Bennis, M., Nam, Y. H., & Debbah, M. (2019). A tutorial on UAVs for wireless networks: Applications, challenges, and open problems. *IEEE communications surveys & tutorials*, *21*(3), 2334-2360. https://doi.org/10.1109/COMST.2019.2902862.

Nguyen, N. T., Nguyen, H. N., Huynh, L. T., & Voznak, M. (2022). Enabling unmanned aerial vehicle to serve ground users in downlink NOMA system. *Bulletin of Electrical Engineering and Informatics*, *11*(6), 3338-3345. https://doi.org/10.11591/eei.v11i6.3945

Sharma, S. K., Bogale, T. E., Chatzinotas, S., Ottersten, B., Le, L. B., & Wang, X. (2015). Cognitive radio techniques under practical imperfections: A survey. *IEEE Communications Surveys and Tutorials*, *17*(4), 1858-1884. https://doi.org/10.1109/COMST.2015.2452414

Shi, W., Zhou, H., Li, J., Xu, W., Zhang, N., & Shen, X. (2018). Drone assisted vehicular networks: Architecture, challenges and opportunities. *IEEE Network*, *32*(3), 130-137. https://doi.org/10.1109/MNET.2017.1700206

Tang, N., Tang, H., Li, B., & Yuan, X. (2020). Cognitive NOMA for UAV-enabled secure communications: Joint 3D trajectory design and power allocation. *IEEE Access*, *8*, 159965-159978. https://doi.org/10.1109/ACCESS.2020.3020821

Yucek, T., & Arslan, H. (2009). A survey of spectrum sensing algorithms for cognitive radio applications. *IEEE communications surveys & tutorials*, *11*(1), 116-130. https://doi.org/10.1109/SURV.2009.090109

Zeng, Y., Zhang, R., & Lim, T. J. (2016). Wireless communications with unmanned aerial vehicles: Opportunities and challenges. *IEEE Communications magazine*, *54*(5), 36-42. https://doi.org/10.1109/MCOM.2016.7470933

Zhang, H., Song, L., Han, Z., & Poor, H. V. (2019). Cooperation techniques for a cellular internet of unmanned aerial vehicles. *IEEE Wireless Communications*, *26*(5), 167-173. https://doi.org/10.1109/MWC.2019.1800591

Zhang, J., Zheng, X., Pan, G., & Xie, Y. (2021). On secrecy analysis of UAV-enabled relaying NOMA systems. *Physical Communication*, *45*, 101263. https://doi.org/10.1016/j.phycom.2020.101263